PHYSICAL REVIEW D **89,** 094512 (2014)

Enumerating copies in the first Gribov region on the lattice in up to four dimensions

Dhagash Mehta[1,2,*] and Mario Schröck[3,†]

[1]*Department of Mathematics, North Carolina State University, Raleigh, North Carolina 27695-8205, USA*
[2]*Department of Chemistry, The University of Cambridge, Lensfield Road, Cambridge CB2 1EW, United Kingdom*
[3]*Istituto Nazionale di Fisica Nucleare (INFN), Sezione di Roma Tre, Rome 00146, Italy*

(Received 14 March 2014; published 29 May 2014)

The covariant gauges are known to suffer from the Gribov problem: even after fixing a gauge nonperturbatively, there may still exist residual copies which are physically equivalent to each other, called Gribov copies. While the influence of Gribov copies in the relevant quantities such as gluon propagators has been heavily debated in recent studies, the significance of the role they play in the Faddeev-Popov procedure is hardly doubted. We concentrate on Gribov copies in the first Gribov region, i.e., the space of Gribov copies at which the Faddeev-Popov operator is strictly positive (semi)definite. We investigate compact U(1) as the prototypical model of the more complicated standard model group SU(N_c). With our graphical processing unit implementation of the relaxation method we collect up to a few million Gribov copies per orbit. We show that the numbers of Gribov copies even in the first Gribov region increase exponentially in two, three and four dimensions. Furthermore, we provide strong indication that the number of Gribov copies is gauge orbit dependent.

DOI: 10.1103/PhysRevD.89.094512 PACS numbers: 12.38.Gc, 11.15.-q, 11.15.Ha

I. INTRODUCTION

The most successful way of studying gauge field theories nonperturbatively is to put them on a finite space-time lattice, and this approach is commonly referred to as lattice field theory [1]. In the continuum, promising nonperturbative approaches are functional methods, in particular Dyson-Schwinger equations (DSEs) [2] and functional renormalization group equations. The DSE approach, for example, can be useful in the low momentum region of quantum chromodynamics (QCD), whereas using lattice QCD one can perform first principles calculations of nonperturbative quantities in QCD. The approximations involved in lattice QCD can be systematically removed,[1] whereas a systematic removal of the truncations in DSEs is much more involved. In other words, lattice simulations can provide an independent check on the results obtained in the DSE approach.

There is, however, a subtle difference in the two approaches. A lattice field theory is manifestly gauge invariant; hence one does not need to fix a gauge on the lattice to calculate gauge invariant observables. In the continuum approaches, each gauge configuration comes with infinitely many equivalent physical copies, the set of which is called a gauge orbit. Hence, to remove the redundant degrees of freedom, one requires gauge fixing. Thus to compare with DSE results, a corresponding gauge fixing is necessary on the lattice.

In the continuum, the standard way to fix a gauge in the perturbative limit is the so-called Faddeev-Popov (FP) procedure [3] which amounts to formulate a gauge fixing device which is called the gauge fixing partition function, Z_{GF}. In the perturbative limit, it can be shown that for an ideal gauge fixing condition, $Z_{\mathrm{GF}} = 1$. Then, this unity is inserted in the measure of the generating functional so that the redundant degrees of freedom are removed after appropriate integration. Becchi, Rouet, Stora and Tyutin (BRST) generalized the FP procedure [4].

Gribov found that in non-Abelian gauge theories a generalized Landau gauge fixing condition, if treated nonperturbatively, has multiple solutions, called Gribov or Gribov-Singer copies [2,5,6]. Thus, the above assumption of the ideal gauge fixing condition became a subtle point in generalizing the FP procedure for nonperturbative field theories. Furthermore, Neuberger showed that on the lattice, the corresponding $Z_{\mathrm{GF}} = 0$ [7,8]; i.e., the expectation value of a gauge fixed observable awkwardly turns out to be $0/0$, known as the Neuberger $0/0$ problem. It yields that BRST formulations cannot be constructed on the lattice, a situation which may severely hamper any comparison of gauge-dependent quantities on the lattice with those in the continuum.

It is argued that Gribov copies may influence the infrared behavior of the gauge dependent propagators of gauge theories both on the lattice [9–11] and in the continuum [12,13]. In [14] SU(2) Yang-Mills theory has been investigated in the strong coupling limit on the lattice: it has been

*dbmehta@ncsu.edu
†mario.schroeck@roma3.infn.it

[1]In practice, due to limited computer power, an extrapolation to the infinite volume and continuum limits has to be performed of which the analytical form is unknown.

shown that the Gribov ambiguity is rather strong in that case and especially affects the ghost propagator. There have also been efforts to count Gribov copies in the continuum in Refs. [15,16] where the counting was restricted for the static spherically symmetric configurations only, for the SU(2) case. Interestingly, recently, a deep relation between lattice gauge fixing and lattice supersymmetry has been proposed [17,18]: the partition functions of a class of supersymmetric Yang-Mills theories can be viewed as a gauge fixing partition function *à la* Faddeev-Popov, and the "Gribov copies" are then nothing but the classical configurations of the theory.

A. Landau gauge on the lattice

On the lattice, gauge fixing is reformulated as an optimization problem. With the gauge fields defined through link variables $U_{i,\mu} \in G$ where the discrete variable i denotes the lattice-site index, $\mu = 1, \ldots, d$ is a directional index and G is the corresponding group of the theory. The standard choice of the lattice Landau gauge (LLG) fixing functional to be optimized with respect to the corresponding gauge transformations $g_i \in G$ is

$$F_U(g) = \sum_{i,\mu} \left(1 - \frac{1}{N_c} \operatorname{Re} \operatorname{Tr} g_i^\dagger U_{i,\mu} g_{i+\hat{\mu}} \right), \tag{1}$$

for $\mathrm{SU}(N_c)$ gauge groups. Choosing $f_i(g) := \frac{\partial F_U(g)}{\partial g_i} = 0$ for each lattice site i gives the lattice divergence of the lattice gauge fields and in the naive continuum limit recovers the continuum Landau gauge condition, i.e., $\partial_\mu A_\mu = 0$, where A_μ is the gauge potential. The corresponding FP operator M_{FP} is then the Hessian matrix of $F_U(g)$ with respect to the gauge transformations. The stationary points of $F_U[g]$ are the Gribov copies.

Neuberger showed [7,8] that when all the stationary points of $F_U[g]$ are taken into account, the gauge fixing partition function Z_{GF} *á la* FP procedure turns out to be zero and the expectation value of a gauge fixed variable is then $0/0$. The Morse theory interpretation of this problem was given by Schaden [19] who showed that Z_{GF} calculates the Euler character χ of the group manifold G at each site of the lattice. In particular, for a lattice with N lattice sites,

$$Z_{\mathrm{GF}} = \sum_i \operatorname{sign}(\det M_{\mathrm{FP}}(g)) = (\chi(G))^N, \tag{2}$$

where the sum runs over all the Gribov copies. Since χ of the group manifold for compact U(1), for S^1, and of the group manifold of $\mathrm{SU}(N_c)$, $S^3 \times S^5 \times \cdots \times S^{2N_c-1}$, is zero, and the corresponding $Z_{\mathrm{GF}} = 0$.

To evade this problem, for an SU(2) gauge theory, Schaden proposed to construct a BRST formulation only for the coset space SU(2)/U(1) for which $\chi \neq 0$. The procedure can be generalized to fix the gauge of an $\mathrm{SU}(N_c)$ lattice gauge theory to the maximal Abelian subgroup $(\mathrm{U}(1))^{N_c-1}$ [20,21]. Thus, the Neuberger $0/0$ problem for an $\mathrm{SU}(N_c)$ lattice gauge theory actually lies in $(\mathrm{U}(1))^{N_c-1}$. For this reason, we concentrate on the compact U(1) case in the rest of the paper.

There are other ways proposed to avoid the Neuberger $0/0$ problem by modifying the gauge fixing condition while taking into account that the corresponding Z_{GF} should be orbit independent, and, for technical convenience, it should be possible to efficiently implement the corresponding gauge fixing numerically. Renormalization, in contrast, is not required: the unitary gauge in gauge-Higgs models, for example, is even perturbatively nonrenormalizable but still yields the correct physics.

In minimal lattice Landau gauge, one focuses on the first Gribov region [22], i.e., the space of minima, in which there is no cancellation among the signs of M_{FP}. Hence, Z_{GF} just counts the number of minima of $F_U[G]$, and the Neuberger $0/0$ is avoided. It is yet to be shown if the corresponding Z_{GF} is orbit independent in general. However, in the one-dimensional [23,24] and two-dimensional [25] compact U(1) cases, it was already shown that Z_{GF} is in fact an orbit-dependent quantity. In the present paper, one of our goals is to verify this in higher dimensional cases.

In absolute lattice Landau gauge, one focuses on the space of global minima, called the fundamental modular region (FMR). The Neuberger $0/0$ problem is again avoided here. It is anticipated that there are no Gribov copies inside the FMR [26,27], which was verified to be true in one- and two-dimensional compact U(1) cases [23–25].

Other approaches to evade the Neuberger $0/0$ problem were recently put forward in [28–37] and reviewed in [38].

B. Lattice Landau gauge for compact U(1)

Following the notations of Ref. [25], for compact U(1) the gauge fields and gauge transformations are $U_{i,\mu} = e^{i\phi_{i,\mu}}$ and $g_i = e^{i\theta_i}$, respectively, where the angles θ_i and $\phi_{i,\mu}$ take values from $(-\pi, \pi]$. Hence, Eq. (1) becomes

$$\begin{aligned} F_\phi(\theta) &= \sum_{i,\mu} (1 - \cos(\phi_{i,\mu} + \theta_{i+\hat{\mu}} - \theta_i)) \\ &\equiv \sum_{i,\mu} (1 - \cos \phi^\theta_{i,\mu}), \end{aligned} \tag{3}$$

where $\phi^\theta_{i,\mu} := \phi_{i,\mu} + \theta_{i+\hat{\mu}} - \theta_i$.

When $\phi_{i,\mu}$ is picked randomly, it is refereed to as a random or *hot* orbit, and when all the ϕ angles are zero, it is called the trivial or *cold* orbit.

We concentrate on periodic boundary conditions, i.e., $\theta_{i+N\hat{\mu}} = \theta_i$ and $\phi_{i+N\hat{\mu},\mu} = \phi_{i,\mu}$, which is the most natural choice in lattice gauge theories. We remove the global gauge degree of freedom by fixing the angle $\theta_{(N,\ldots,N)}$ to zero. Furthermore, we let $\{\phi_{i,\mu}\}$ take random values independent of the action, corresponding to the strong coupling limit $\beta = 0$, which is sufficient to answer the basic

questions of counting Gribov copies and their orbit dependence as every gauge orbit has a nonvanishing weight for any finite β. The global minimum of $F_\phi(\theta)$ is usually thought to be unique modulo possible accidental degeneracies which are expected to form a set of measure zero (and nonaccidental degeneracies on the boundary of the FMR). Therefore, we focus on the minimal lattice Landau gauge in this work.

II. WHAT IS KNOWN SO FAR

All the Gribov copies for the one-dimensional LLG for compact U(1) have been found analytically for periodic [23,24] and antiperiodic [23,28,29] boundary conditions. However, solving the stationary equations in more than one dimension turns out to be a difficult task and has not been done so far. The main difficulty here is that the stationary equations are highly nonlinear in higher dimensions. In Ref. [23] it was shown how these equations could be viewed as a system of polynomial equations, and then the numerical polynomial homotopy continuation method was used to find all the stationary points for small lattices in two dimensions. The method was used extensively afterwards to study similar problems of finding stationary points or minima of a multivariate function arising in statistical mechanics and particle physics [25,39–51]. Interestingly, in Ref. [43], two types of singular solutions were observed for the trivial orbit case: isolated singular solutions at which the Hessian matrix is singular (these solutions are in fact multiple solutions) and a continuous family of singular solutions. It was shown that one can construct one-, two-, etc., parameter solutions, even after fixing the global $O(2)$ freedom.

The authors of [52] studied the continuum limit of lattice U(1) theory in two dimensions and found that in that limit, the absolute and local minima become more and more degenerate.

In Ref. [25], for the two-dimensional case, among other results using the conjugate gradient method it was conjectured that the number of Gribov copies in the first Gribov region increases exponentially. In Refs. [53,54], the problem of finding minima of the compact U(1) LLG in two dimensions was studied for the trivial orbit case, which is nothing but the two-dimensional XY model without disorder. There, many minima were found using potential energy landscape methods [55,56], and it was shown that the number of minima increased exponentially in this case. Moreover, using disconnectivity diagrams, it was shown how the minima were connected to each other via the saddles of index 1 (called transition states in theoretical chemistry). In the current paper, we want to verify this conjectured exponential increase in three and four dimensions. As a by-product, we also improve on the previous results for two dimensions. In a separate work, we develop a novel and efficient method to find many Gribov copies, if not all, starting from a maximum of the lattice Landau gauge fixing functional and moving toward lower index saddles [57].

III. A GPU IMPLEMENTATION OF THE RELAXATION METHOD

In this section we describe our numerical approach. We adopt the relaxation algorithm and execute it on graphics processing units (GPUs) which offer a high level of parallelism and thus enable us to gather a large number of samples within a practical amount of computer time.

The idea of the relaxation algorithm is to sweep over the lattice while optimizing the gauge functional (1) locally on each lattice site. Thus, on each site i the maximum of

$$\frac{1}{2}\,\mathrm{Re}[g_i K_i] \tag{4}$$

is to be found. Here we introduced

$$K_i \equiv \sum_\mu [U_{i,\mu} g^\dagger_{i+\hat{\mu}} + U^\dagger_{i-\hat{\mu},\mu} g^\dagger_{i-\hat{\mu}}]. \tag{5}$$

It is easy to see that Eq. (4) becomes maximized if we simply set θ_i equal to the phase of K_i^*.

Note that the local optimization depends for each lattice site on the nearest neighbors only; hence we can perform a checkerboard decomposition of the lattice, and the local optimization of all lattice sites of one of the two sublattices will be independent of all other lattice sites of the same sublattice. Our implementation will benefit therefrom by optimizing all lattice sites of a given sublattice concurrently instead of performing serial loops over the members of each sublattice. We do not perform overrelaxation since we have found that, while overrelaxation decreases the convergence time, it also decreases the chance of converging to larger minima and thus introduces a bias.

NVIDIA offers with CUDA (Compute Unified Device Architecture) a parallel programming model that enables the programmer to run so-called kernels on the GPU. These kernels are specialized functions that perform a sequence of tasks in a highly parallel fashion. The user defines a grid of thread blocks and a number of threads per thread block in such a way that the kernel call replaces serial loops over memory addresses by concurrent calculations on all corresponding addresses.

Our implementation is based on the CULGT[2] code for lattice gauge fixing on GPUs [58]. Here we assign one thread to one lattice site, and a whole lattice will be encapsulated in one thread block. The GPU can handle several thread blocks per multiprocessor concurrentl, and we launch a grid of thread blocks where each thread block contains a lattice initialized with random numbers which we generate with the PHILOX random number

[2]http://www.cuLGT.comURL.

TABLE I. The number of orbits and the number of samples per orbit for each lattice size N^d for which we have minimized the gauge functional. The average number of distinct minima that we collected and the corresponding standard deviation is listed.

	$d=2$					$d=3$			$d=4$	
N	2	4	6	8	10	2	4	6	2	4
No. orbits	100	100	100	100	10	100	100	3	100	1
No. samples/orbit $[1024^2]$	4	4	4	16	256	4	4	1024	4	1024
Avg. no. of minima	1.1	4.7	66.2	2,464	185,709	1.8	394.7	3.335×10^6	4.5	2.774×10^6
Std. dev.	0.3	2.2	35.1	1,618	110,779	0.9	228.3	79,529.0	2.4	⋯

generator [59]. In this way we minimize in parallel as many samples as we launch thread blocks. Moreover, we add another layer of parallelism by adopting multiple GPUs: therefore we loop over the kernel calls in the main function of the execution code while switching between the multi-GPUs.

In practice we adopt four cards of the NVIDIA Tesla C2070, and we launch 1024 thread blocks (i.e., random start samples) per GPU. Hence we run 4096 samples at once. While CUDA allows for a much larger number of thread blocks to be launched per kernel call, this can be counterproductive since the runtime depends on the slowest converging sample among all running samples. A smaller number than 1024 thread blocks per GPU, on the other hand, would not fully occupy the GPU and thus result again in a performance loss. Therefore, we keep the grid size as 1024 blocks per GPU fixed. For each sample we store the value of the minimum to which the relaxation algorithm has converged and subsequently sort these values via bitonic sort, again accelerated by the GPU.

The execution time of the code depends on the lattice size and the number of iterations until convergence which varies from sample to sample. In practice, the time to minimize one *mebisample* (1024^2 samples) adopting four NVIDIA Tesla C2070 GPUs varies from a few seconds (e.g., $d=2$ up to $N=6$ lattices) over several minutes (e.g., 10^2 and 4^3) up to a few hours (8^3 and 4^4).

As a stopping criterion we require the largest gradient over all lattice sites and all concurrently running samples to be smaller than 10^{-12}. We have found that this criterion is sufficient to ensure that the values of the minima to which the relaxation algorithm converges to reach plateaus to a precision of at least 10^{-10}. The whole simulation is performed in double precision, and we store the values of the minima in double precision.[3] Subsequently we transform each minimum $x \in [0, 1.0]$ to an integer $X \in [0, 10^8]$. These integers can then be unambiguously compared using the bitonic sort algorithm. The inverse of the upper bound of the integer interval defines the resolution with which we choose to distinguish minima.

[3]In [58] it was shown that the accumulation of numerical errors of typical observables in double precision in lattice gauge fixing is smaller than 10^{-12} even for extensively long simulation runs.

Hence we consider values of minima as the same when they agree within eight decimal places. It is likely that with our resolution of 10^{-8} we count some minima as the same which are distinct at finer resolution; i.e., finer resolution may eventually allow higher distinction of otherwise non-distinguishable minima. Adopting this rather conservative resolution we assure that we obtain real lowest bounds of the number of Gribov copies per orbit which has the highest priority for our study. More details on the numerical distinction of Gribov copies, including a discussion of renormalization effects, can be found in [60].

In the present work, we sample orbits randomly; i.e., we consider the theory at the strong coupling limit where the inverse coupling $\beta = 0$. This choice of β is sufficient to make general conclusions for the number of Gribov copies for the purpose of this work.

IV. RESULTS

A. Number of Gribov copies

In Table I we list for each lattice size the number of orbits and the number of samples per orbit for which we have minimized the gauge functional Eq. (1). Note that the number of samples is given in units of *mebisample* (1024^2 samples).

In Figs. 1–3 we plot the number of distinct minima that we found as a function of the number of random initial guesses. Because of the nature of the bitonic sorting algorithm, we measure the number of minima only at stages of powers of two in the number of samples. In the figures, the resulting points are connected by straight lines to guide the eye.

In two dimensions (Fig. 1), we find for $N=6$ that all orbits have converged to plateaus, indicating that we are very close to having found all minima in that case. Similarly, the plot for $N=8$ (same figure) reveals that still a relatively large fraction of the orbits have converged. The curves in the plot for $N=10$, in contrast, have not converged, and consequently we are further away from having collected all minima here. Analogously, Fig. 2 shows the data for $d=3$ where we reach our limit for $N=6$: one gibisample (1024^3 samples) per orbit is not sufficient to get close to finding all minima. In four dimensions, we sample one hundred 2^4 orbits and a single orbit of $N=4$ with a gibisample initial guesses for which we obtain only a relatively weak lower bound on the number of distinct minima.

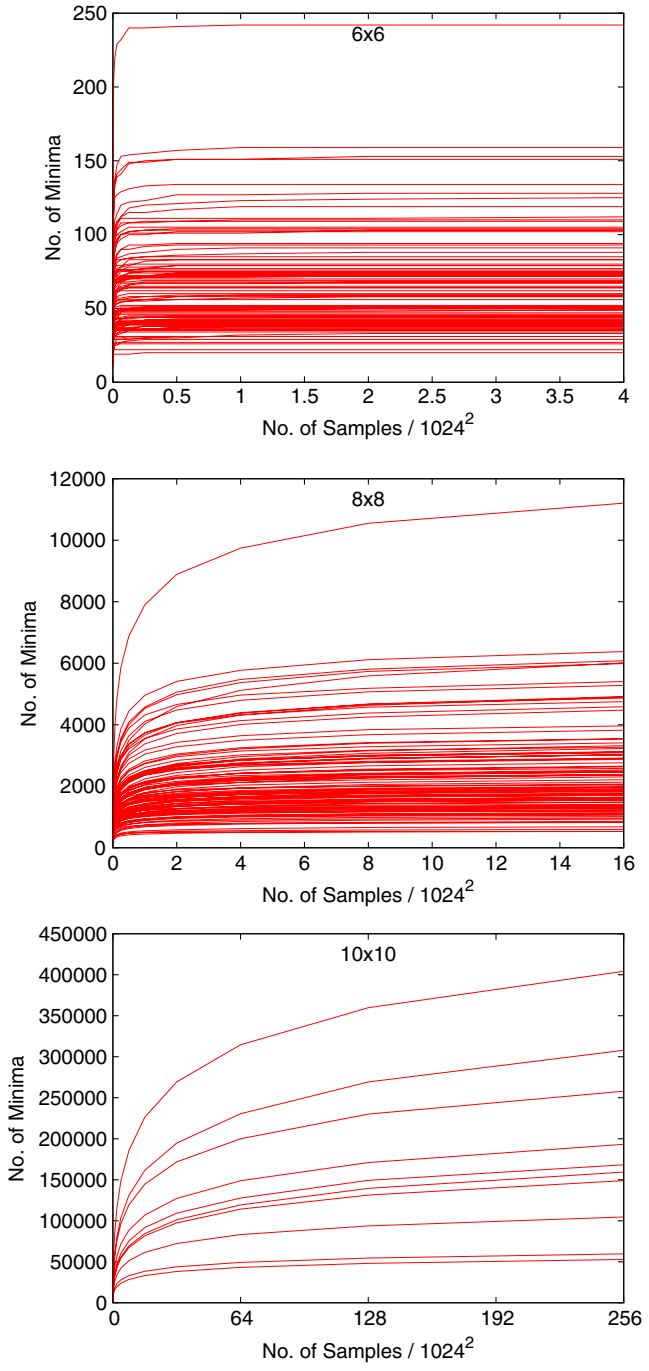

FIG. 1 (color online). The number of distinct minima versus the number of samples (initial guesses) for different orbits for $d = 2$ and $N = 6, 8, 10$.

We conclude that even though we have not found every single minimum for each orbit, Figs. 1–3 provide clear evidence that the number of Gribov copies is orbit dependent.

The averages and standard deviations for the lower bounds of the number of minima per orbit and lattice size are summarized in Table I. The lower bounds on the

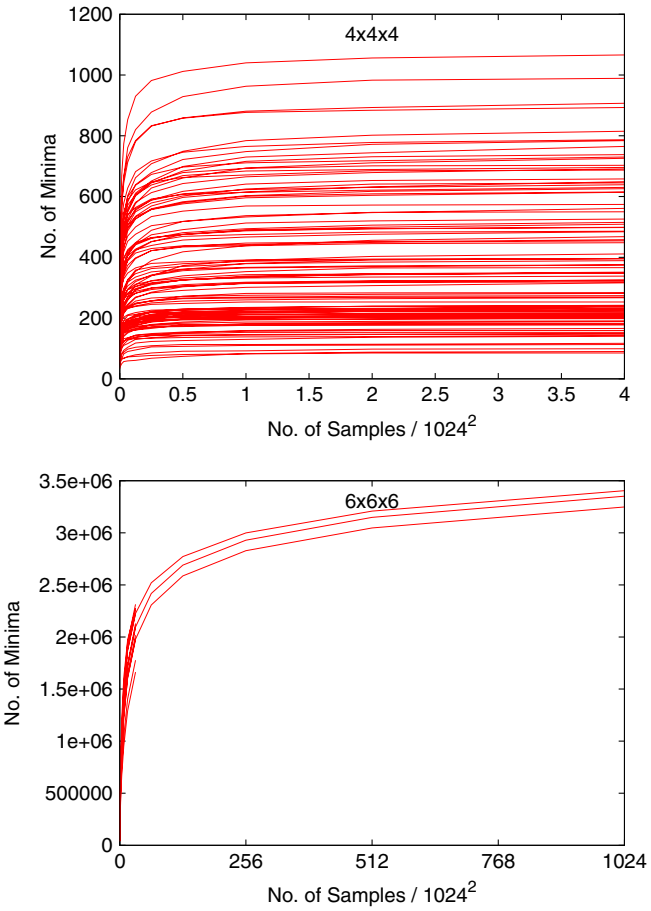

FIG. 2 (color online). The number of distinct minima found versus the number of samples (random starts) for the three different orbits for $d = 3$ and $N = 4, 6$.

number of minima as a function of N for all dimensions is plotted in Fig. 4. Additionally, best fits to a function

$$h(x) = a \exp\left(bx^c\right) \tag{6}$$

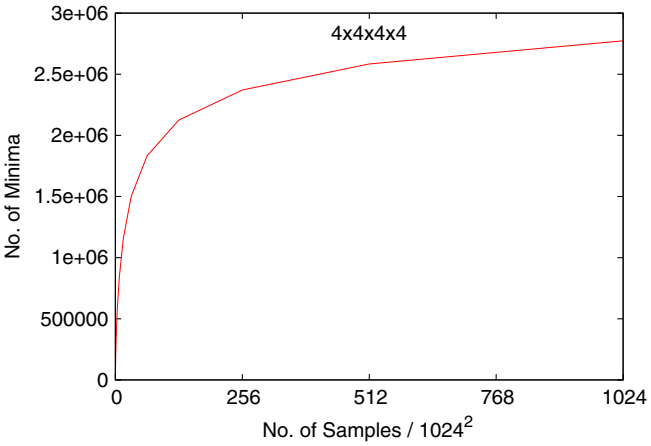

FIG. 3 (color online). The number of distinct minima found versus the number of samples (random starts) for a single orbit under investigation for $d = 4$ and $N = 4$

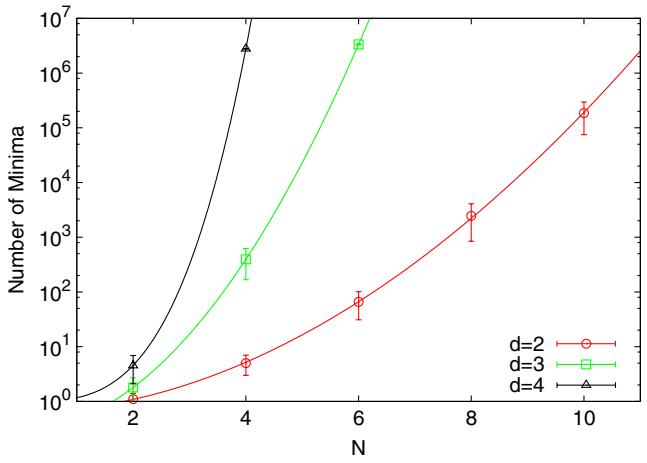

FIG. 4 (color online). Lower bounds of the number of minima as a function of N for $d = 2, 3, 4$ averaged over the different random orbits. The curves correspond to best fits to the function Eq. (6), and the corresponding fit parameters are summarized in Table II.

are shown, and the corresponding fit parameters are listed in Table II. The data for $d = 2$ indicate that the number of distinct gauge functional minima depends exponentially on N^2. The data for $d = 3$ do not confirm an exponent N^d, but this is probably because our lowest bound for 6^3 severely underestimates the true number of copies.[4]

B. The values of the gauge functional at the minima and their distribution

To investigate how many mebisamples we need to sufficiently sample nearly all minima with reasonable statistics, we compare the set of minima we obtained from ten orbits of a 10^2 lattice from 4 mebisamples per orbit to the set of minima when we apply 256 mebisamples per orbit to the same ten orbits. We assign each minimum to a bin of resolution 10^{-4} and plot the ratios of the entries of the bins from 256 versus 4 mebisamples in Fig. 5. The plot reveals that the ratios of the low-lying and midrange minima are very close to the expected factor 256/4, whereas the ratios fluctuate much stronger for high-lying minima. Moreover, only very high-lying bins of the 4 mebisample run are empty while the corresponding bins of the 256 mebisample run have entries, as presented in the lower plot of the figure. This indicates that 4 mebisamples are sufficient to obtain reasonable statistics and running more samples will improve mainly in the range most distant to the global minimum which appears to be less attractive for the relaxation algorithm.

With the aim of studying the dependence of the value of the gauge functional at the global minimum on N and d, it is desirable to investigate more orbits to increase the statistics. Motivated by the conclusion of the previous paragraph, we limit the number of samples per orbit to 4 mebisamples which renders increasing the number of orbits affordable. Nevertheless we are confident that the smallest minimum we find on each orbit is at least numerically very close to the global minimum, if not equal to it. Hence we study the global minima of the orbits listed in Table III which additionally include 8^3 lattices.

[4]The $N = 6$ curves in Fig. 1 are still rising by more then 6% when increasing the number of samples from 512 to 1024 mebisamples. Moreover, the three curves are rather close to each other compared to, e.g., the curves for $N = 4$.

TABLE II. The fit parameters of the curves Eq. (6) shown in Fig. 4.

Dim	a	b	c
2	0.631(38)	0.141(11)	1.953(33)
3	0.305(-)	0.440(-)	2.012(-)
4	1 (fixed)	0.156(-)	3.287(-)

In Fig. 6, the gauge functional Eq. (1) evaluated at the global minimum as a function of N for $d = 2, 3, 4$ is shown. For constant N, the value of the global minimum is higher for higher dimension d, and for fixed d the global minima seem to converge to plateaus for $N \gtrsim 6$.

In Fig. 7 histograms for the distribution of the functional values for all lattice sizes, the superimposing data from all orbits of Table III are shown. It is evident that the distribution becomes narrower with increasing lattice size N. It is important to stress, however, that the wide spread for lower N is mainly due to the large variance of the value of the global minimum; compare with the data in the table. Figure 8, in contrast, shows the distribution of the minima F_i relative to the global minimum F_g on that orbit:

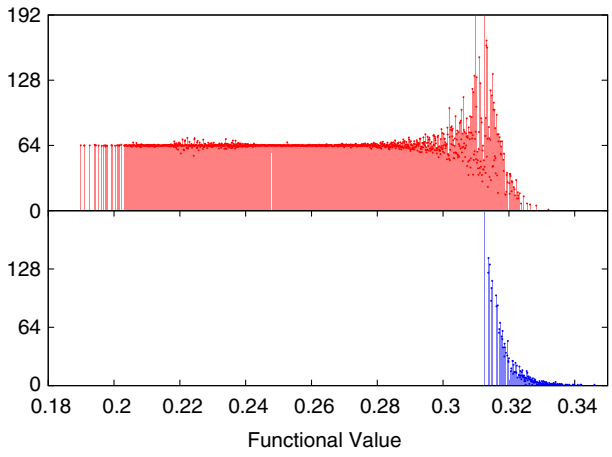

FIG. 5 (color online). In the upper part of the plot we show the ratio of each of the bins (resolution 10^{-4}) of the distribution of the histograms of the minima of ten orbits of a 10^2 lattice, taking 256 versus 4 mebisamples into account. The lower part of the plot shows the bins from 256 mebisamples when the corresponding bin of 4 mebisamples was empty (i.e., the ratio in the upper plot was not defined). Points on top of the bin bars are plotted for better visibility.

TABLE III. A complementary set of gauge functional minima: more orbits per lattice size with four mebisamples (4,194,304 samples) per orbit. The averages of the values of the gauge functional at the global minimum and the corresponding standard deviations are listed (cf. Fig. 6).

	$d=2$					$d=3$				$d=4$	
N	2	4	6	8	10	2	4	6	8	2	4
Number of orbits			100				100		20	100	7
Average global minimum F	0.431	0.249	0.219	0.210	0.208	0.441	0.338	0.328	0.324	0.482	0.413
Standard deviation	0.139	0.037	0.022	0.016	0.014	0.076	0.014	0.006	0.005	0.045	0.006

$(F_i - F_g)/F_g$. Subsequently, the data have been averaged over all orbits. As a consequence of this strategy, the aforementioned effect of the variance of the global minima is factored out. The deviation (Fig. 8) appears to increase with N, not decrease as it should if global and local minima became equivalent. In summary, our data do not indicate that global and local minima become equivalent for large N (in the strong coupling limit).

V. CONCLUSIONS

On the lattice, gauge fixing is formulated as a minimization problem. The stationary points of the gauge fixing functional are the Gribov copies which are physical replications of a gauge configuration and exist even after fixing the gauge nonperturbatively. In this paper, we aimed at enumerating the number of Gribov copies in the first Gribov region on the lattice in order to address different modifications of the gauge fixing procedure which can be affected by the potential orbit dependence of the number of Gribov copies. We studied compact U(1) gauge theory. The latter not only can serve as a laboratory for testing our computational efforts, but it is a very important model in its own right: it has been shown that the origin of the Neuberger 0/0 problem lies in compact U(1), and the problem is evaded for any SU(N) when it is evaded for

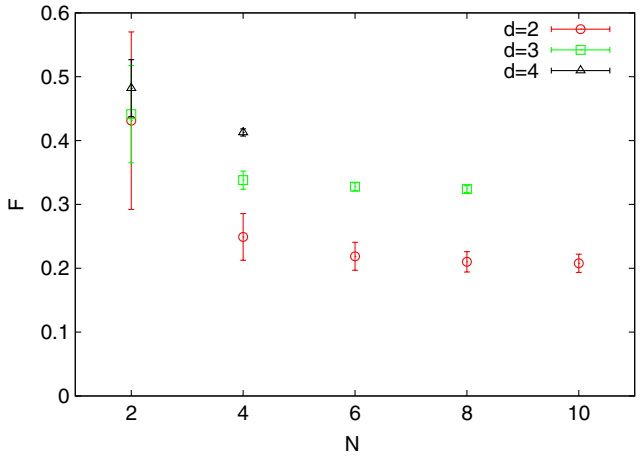

FIG. 6 (color online). The gauge functional evaluated at the global minimum as a function of N for $d = 2, 3, 4$.

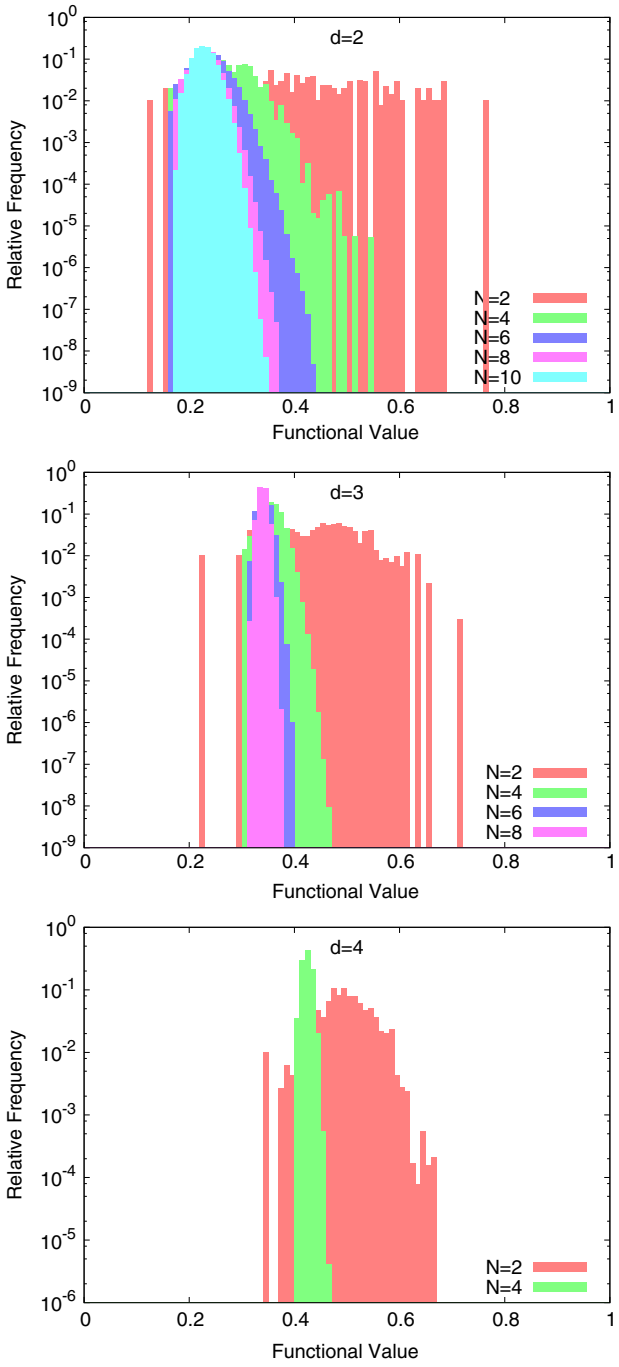

FIG. 7 (color online). The normalized distribution of the minima of all orbits and samples of $d = 2, 3, 4$ (see Table III).

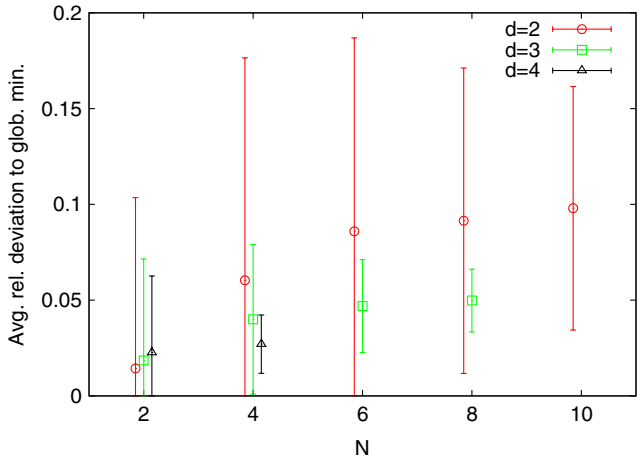

FIG. 8 (color online). The averages and standard deviations of the relative deviation of the local minima F_i from the global minimum F_g on the corresponding orbit: $(F_i - F_g)/F_g$.

compact U(1). This holds even though Gribov copies in the compact U(1) case are just lattice artifacts.

We performed a brute force analysis of the first Gribov region for the compact U(1) case in $d = 2, 3, 4$ dimensions. We started the relaxation algorithm from up to more than a billion random points on the gauge orbits and collected up to millions of distinct gauge functional minima per orbit. Even though our GPU implementation has proven to be a powerful tool for counting Gribov copies, we observed that the problem of counting Gribov copies becomes increasingly difficult with increasing lattice sizes. In particular, for the biggest volumes of our runs (10^2, 6^3 and 4^4), the convergence to the full number of distinct minima with an increasing number of minimization attempts ("samples") could not be achieved. In $d = 4$ we reached our limits with a single orbit of the modest lattice size 4^4.

We were able to show that the number of Gribov copies in the first Gribov region increases exponentially in two, three and four dimensions. More specifically, we found that the number of distinct minima per orbit increases at least with $\exp(\sim N^2)$ and that an $\exp(\sim N^d)$ dependence is likely, though it could not definitely be shown with the currently available data. Moreover, we have found a strong indication that the number of minima is orbit dependent, i.e., a strong indication that the gauge fixing partition function for the minimal Landau gauge on the lattice is orbit dependent.

Finally, in the continuum it was conjectured that the local minima of the corresponding gauge fixing functional tend to be degenerate with the global minimum [22]. A direct comparison with this conjecture cannot be done using our results on the lattice with $\beta = 0$. However, while our data exhibit narrowing of the distribution of the values of the gauge fixing functional at the minima when increasing the lattice size (taking data from several orbits per lattice size into account), we cannot observe that local minima tend to get closer to the global minimum of the corresponding orbit.

ACKNOWLEDGMENTS

The authors are very grateful to Reinhard Alkofer, Maartin Golterman, Axel Maas, Jonivar Skullerud, Martin Schaden, and Yigal Shamir for helpful discussions and comments on the manuscript. D. M. was supported by an ERC and a DARPA Young Faculty Award. The calculations have been performed on the "mephisto" cluster at the University of Graz.

[1] H. J. Rothe, World Sci. Lect. Notes Phys. **82**, 1 (2012).
[2] R. Alkofer and L. von Smekal, Phys. Rep. **353**, 281 (2001).
[3] L. Faddeev and V. Popov, Phys. Lett. **25B**, 29 (1967).
[4] C. Becchi, A. Rouet, and R. Stora, Ann. Phys. (N.Y.) **98**, 287 (1976).
[5] V. Gribov, Nucl. Phys. **B139**, 1 (1978).
[6] I. Singer, Commun. Math. Phys. **60**, 7 (1978).
[7] H. Neuberger, Phys. Lett. B **175**, 69 (1986).
[8] H. Neuberger, Phys. Lett. B **183**, 337 (1987).
[9] R. Aouane, V. G. Bornyakov, E.-M. Ilgenfritz, V. K. Mitrjushkin, M. Müller-Preussker, and A. Sternbeck, Phys. Rev. D **85**, 034501 (2012).
[10] V. Bornyakov, V. Mitrjushkin, and R. Rogalyov, Phys. Rev. D **86**, 114503 (2012).
[11] A. Cucchieri, Nucl. Phys. **B508**, 353 (1997).
[12] A. Ilderton, M. Lavelle, and D. McMullan, *Proc. Sci.*, QCD-TNT09 (**2007**) 019.
[13] A. Ilderton, M. Lavelle, and D. McMullan, J. High Energy Phys. 03 (2007) 044.
[14] A. Maas, J. M. Pawlowski, D. Spielmann, A. Sternbeck, and L. von Smekal, Eur. Phys. J. C **68**, 183 (2010).
[15] B. Holdom, Phys. Rev. D **78**, 125030 (2008).
[16] B. Holdom, Phys. Rev. D **79**, 085013 (2009).
[17] S. Catterall, R. Galvez, A. Joseph, and D. Mehta, J. High Energy Phys. 01 (2012) 108.
[18] D. Mehta, S. Catterall, R. Galvez, and A. Joseph, *Proc. Sci.*, LATTICE2011 (**2011**) 078.
[19] M. Schaden, Phys. Rev. D **59**, 014508 (1998).
[20] M. Golterman and Y. Shamir, Phys. Rev. D **87**, 054501 (2013).
[21] M. Golterman and Y. Shamir, Phys. Rev. D **70**, 094506 (2004).
[22] D. Zwanziger, Nucl. Phys. **B323**, 513 (1989).
[23] D. Mehta, Ph.D. thesis, The University of Adelaide, 2009.

[24] D. Mehta and M. Kastner, Ann. Phys. (Amsterdam) **326**, 1425 (2011).
[25] C. Hughes, D. Mehta, and J.-I. Skullerud, Ann. Phys. (Amsterdam) **331**, 188 (2013).
[26] D. Zwanziger, Nucl. Phys. **B412**, 657 (1994).
[27] P. van Baal, *Confinement, Duality and Non-perturbative Aspects of QCD* (Newton Institute, Cambridge, UK, 1997), pp. 161-178.
[28] L. von Smekal, D. Mehta, A. Sternbeck, and A. G. Williams, *Proc. Sci.*, LAT2007 (**2007**) 382.
[29] L. von Smekal, A. Jorkowski, D. Mehta, and A. Sternbeck, *Proc. Sci.*, CONFINEMENT8 (**2008**) 048.
[30] L. von Smekal, arXiv:0812.0654.
[31] M. Testa, Phys. Lett. B **429**, 349 (1998).
[32] A. Maas, Phys. Lett. B **689**, 107 (2010).
[33] A. Maas, *Proc. Sci.*, ConfinementX (**2012**) 034.
[34] A. Kalloniatis, L. von Smekal, and A. Williams, Phys. Lett. B **609**, 424 (2005).
[35] M. Ghiotti, L. von Smekal, and A. Williams, AIP Conf. Proc. **892**, 180 (2007).
[36] L. von Smekal, M. Ghiotti, and A. G. Williams, Phys. Rev. D **78**, 085016 (2008).
[37] D. Mehta, N. Daleo, J. Hauenstein, and C. Seaton (unpublished).
[38] A. Maas, Phys. Rep. **524**, 203 (2013).
[39] D. Mehta, A. Sternbeck, L. von Smekal, and A. G. Williams, *Proc. Sci.*, QCD-TNT09 (**2009**) 025.
[40] D. Mehta, Phys. Rev. E **84**, 025702 (2011).
[41] D. Mehta, Adv. High Energy Phys. **2011**, 1 (2011).
[42] M. Kastner and D. Mehta, Phys. Rev. Lett. **107**, 160602 (2011).
[43] R. Nerattini, M. Kastner, D. Mehta, and L. Casetti, Phys. Rev. E **87**, 032140 (2013).
[44] D. Mehta, J. D. Hauenstein, and M. Kastner, Phys. Rev. E **85**, 061103 (2012).
[45] M. Maniatis and D. Mehta, Eur. Phys. J. Plus **127**, 91 (2012).
[46] D. Mehta, Y.-H. He, and J. D. Hauenstein, J. High Energy Phys. 07 (2012) 018.
[47] J. Hauenstein, Y.-H. He, and D. Mehta, J. High Energy Phys. 09 (2013) 083.
[48] B. Greene, D. Kagan, A. Masoumi, D. Mehta, E. J. Weinberg, and X. Xiao, Phys. Rev. D **88**, 026005 (2013).
[49] D. Mehta, D. A. Stariolo, and M. Kastner, Phys. Rev. E **87**, 052143 (2013).
[50] D. Martinez-Pedrera, D. Mehta, M. Rummel, and A. Westphal, J. High Energy Phys. 06 (2013) 110.
[51] Y.-H. He, D. Mehta, M. Niemerg, M. Rummel, and A. Valeanu, J. High Energy Phys. 07 (2013) 050.
[52] P. de Forcrand and J. E. Hetrick, Nucl. Phys. B, Proc. Suppl. **42**, 861 (1995).
[53] D. Mehta, C. Hughes, M. Schröck, and D. J. Wales, J. Chem. Phys. **139**, 194503 (2013).
[54] D. Mehta, C. Hughes, M. Kastner, and D. J. Wales (unpublished).
[55] D. Wales, *Energy Landscapes: Applications to Clusters, Biomolecules and Glasses*, Cambridge Molecular Science (Cambridge University Press, Cambridge, UK, 2004).
[56] M. Kastner, Rev. Mod. Phys. **80**, 167 (2008).
[57] D. Mehta, C. Hughes, and D. J. Wales, J. Chem. Phys. (to be published).
[58] M. Schröck and H. Vogt, Comput. Phys. Commun. **184**, 1907 (2013).
[59] J. K. Salmon, M. A. Moraes, R. O. Dror, and D. E. Shaw, in *Proceedings of 2011 International Conference for High Performance Computing, Networking, Storage and Analysis, SC '11* (ACM, New York, 2011), p. 16.
[60] A. Maas, *Proc. Sci.*, QCD-TNT-II (**2011**) 028.